AMERICAN JOURNAL OF PHYSICAL ANTHROPOLOGY 143:52–61 (2010)

Waddling and Toddling: The Biomechanical Effects of an Immature Gait

Libby W. Cowgill,[1]* Anna Warrener,[2] Herman Pontzer,[2] and Cara Ocobock[2]

[1]*Department of Anthropology, University of Central Florida, Orlando, FL 32816-1361*
[2]*Department of Anthropology, Washington University, St. Louis, MO 63130*

KEY WORDS femur; ground reaction force; shape; walking

ABSTRACT Femoral shape changes during the course of human growth, transitioning from a subcircular tube to a teardrop-shaped diaphysis with a posterior pilaster. Differences between immature and mature bipedalism and body shape may generate different loads, which, in turn, may influence femoral modeling and remodeling during the course of the human lifespan. This study uses two different approaches to evaluate the hypotheses that differences in gait between young and mature walkers result in differences in ground reaction forces (GRFs) and that the differences in loading regimes between young children and adults will be reflected in the geometric structure of the midshaft femur. The results of this analysis indicate that GRFs differ between young walkers and adults in that normalized mediolateral (ML) forces are significantly higher in younger age groups. In addition, these differences between children and adults in the relative level of ML bending force are reflected in changes in femoral geometry during growth. During the earlier stages of human development, immature femoral diaphyses are heavily reinforced in approximately ML plane. The differences in gait between mature and immature walkers, and hence the differences in femoral shape, are likely partially a product of a minimal bicondylar angle and relatively broad body in young children. Am J Phys Anthropol 143:52–61, 2010.

Midshaft femoral shape has been used frequently to infer levels of terrestrial mobility both within and among archaeological and paleoanthropological populations (Ruff, 1987; Larsen, 1997; Stock and Pfeiffer, 2001, 2004; Holt, 2003; Wescott, 2006; Shackelford, 2007). Based on experimental studies of bone strain during human walking (Morrisson, 1969; Paul, 1971; Lanyon et al., 1975), researchers have argued that the elevated anteroposterior (AP) reinforcement evident in the lower limb of some populations is the result of increased AP bending loads related to greater mobility (Ruff, 2000; Wescott, 2006; Shackelford, 2007; Shaw and Stock, 2009).

However, differences in long bone shape have also been linked to the manner, as opposed to the frequency, of mechanical loading (Ruff, 1995; Trinkaus, 1997; Ruff et al., 2006; Richmond and Jungers, 2008). Ruff (1995) suggested that differences in femoral shaft shape and morphology among hominin populations reflect differences in pelvic and proximal femoral anatomy. In this model, a suite of functionally related characteristics, including an elongate femoral neck and increased biacetabular breadth, lead to the generation of elevated mediolateral (ML) bending forces around the femoral diaphysis. This functional model has since been used to provide insight into femoral morphology among early hominins (Richmond and Jungers, 2008), Neandertals (Trinkaus, 1997) and the Tyrolean "Iceman" (Ruff et al., 2006).

If changes in the manner of loading can affect midshaft femoral shape, it follows that femoral geometric structure should change during the course of ontogeny, as normal human gait and body proportions differ between adults and younger individuals. Human bipedalism does not become completely mature until at least 4 or 5 years of age (McGraw, 1940; Statham and Murray, 1971), and until that age, various factors in children such as stance, step length, cadence, and walking velocity differ from the patterns seen in adults (Sutherland et al., 1980, 1988). Early walking in toddlers is typified by a wide stance with an abducted thigh, flexion of the knee and hip, abducted arms, and extended elbows (McGraw, 1940; Okamoto and Okamoto, 2007). As gait matures, stance width diminishes, normal arm swing appears, and step length and walking velocity increase (Sutherland et al., 1980). Furthermore, pathological deviation from these normal gait patterns during growth leads to abnormal skeletal development (Carriero et al., 2009).

It is possible, therefore, that normal changes in gait patterns across ontogeny are linked to changes in long bone shape during growth. The type of biomechanical loading produced during early walking likely differs from that of mature gait, and differences between the loads engendered during the two different types of bipedality may result in differential modeling of the lower limb in young children and adults.

Grant sponsors: Leakey Foundation, Wenner-Gren Foundation, National Science Foundation; Grant number: NSF BCS-0549925.

*Correspondence to: Libby W. Cowgill, Department of Anthropology, University of Central Florida, 4000 Central Florida Boulevard, Howard Phillips Hall, 309, Orlando, FL 32816-1361.
E-mail: lcowgill@mail.ucf.edu

Received 27 August 2009; accepted 25 January 2010

DOI 10.1002/ajpa.21289
Published online 22 March 2010 in Wiley InterScience (www.interscience.wiley.com).

RESEARCH HYPOTHESES

Given this, our analysis uses two different forms of biomechanical data to test three hypotheses. First, primarily because of differences in gait, ground reaction forces (GRFs) change during ontogeny. Relative ML and AP force components will differ between young walkers and adults because of differences in locomotion. Second, differences in loading regimes between young children and adults will be reflected in the geometric structure of the midshaft femur. Third, ground force reaction and femoral structural geometry will correlate during the course of ontogeny.

MATERIALS AND METHODS

Analysis of ground reaction forces

GRF data for this study were obtained from 13 children and 10 adults. Human subject participation was approved by the Human Research Protection Office, Washington University in St. Louis, and informed consent was obtained from each participant or participant's guardian before participation. Subjects walked barefoot at self-selected, "normal" speeds along a 10 foot (children) or 20 foot (adults) trackway with an embedded forceplate (AMTI, model OR-6, operating at 1000 or 4000 Hz). Reflective markers were adhered to the skin overlying the greater trochanter, lateral femoral condyle, and lateral malleolus, and these markers were tracked using high speed infrared cameras (Vicon MX4, 200 fps). Vicon Nexus 3.1 software was used to record vertical (Z), AP, and ML GRF. The net AP impulse and average forward velocity were used to determine the percentage change in speed during the step (i.e., acceleration or deceleration). Successful trials were defined as those in which the subject's speed changed less than 20% during the trial, and in which the subject placed only one foot completely on the force plate during the trial. For the adults (n = 10) and many children (n = 6), two or three trials met these criteria. However, the velocity-change criterion eliminated all but one trial for several (n = 7) of the child subjects. Therefore, we examined GRF patterns in the most conservative sample of trials and in an expanded sample that included trials in which velocity change was more than 20%. Both samples gave similar results.

We measured both peak GRF and GRF impulse (i.e., mean GRF magnitude) for all trials. GRF magnitude increases at greater speeds and with greater body mass as the time available to produce the required ground force decreases and bodyweight increases (Pontzer, 2005). Therefore, to account for the effects of walking speed and body size across adults and children, we examined ratios of AP/ML, ML/Z, and AP/Z GRF. Peak GRF was calculated using the maximum force value for that plane (e.g., peak A or peak P/peak M or peak L). For adults, peak force along the AP axis was anterior in nine subjects and posterior in one subject, whereas peak force along the ML axis was medial in eight subjects and lateral in two subjects. For children, peak force in the AP plane was anterior in four subjects and posterior in nine subjects, whereas peak force in the ML plane was medial in 10 subjects and lateral in three subjects. GRF impulses were calculated as the mean absolute value of the GRF trace in each plane.

We also examined speed and limb position to test whether differences in GRF patterns might be a function of differences in speed, or whether differences in limb segment position might differentially affect the relationship between GRF patterns and bending moments in the lower limb. Speeds were compared using Froude number, a size-corrected speed (Alexander, 1984) calculated as velocity^2/(hip height $\times$ gravity) for each trial, and plotting GRF ratios against Froude number to determine whether size-corrected speed and GRF patterns are related. Limb segment angles were calculated using the position of reflective markers adhered to the skin over the greater trochanter, lateral femoral condyle, and lateral malleolus. Segment angles were measured in the sagittal (AP) plane at heel strike and toe-off, and in the coronal (ML) plane at midstance. For GRF, Froude number, and limb segment angle comparisons, mean values for each subject were calculated and Student's t tests were used to compare between three age categories: 1.0–3.9 years (n = 10), 4.0–8.9 years (n = 3), and 18–35 years (adults, n = 10). Because of the small number of trials with adequate kinematic data for older children (4.0–8.9 years), comparisons of limb segment angles were limited to younger children (1.0–3.9 years) and adults.

Analysis of midshaft femoral shape

The primary data for the analysis of femoral shape consist of midshaft femoral cross-sectional properties from seven modern human (Holocene) skeletal samples (Cowgill, 2010). Cross-sectional geometric properties from a total of 521 right and left femora were collected from immature individuals under the age of 18 years. A single femur was selected from each individual based on preservation; the low level of lower limb strength asymmetry makes high levels of nonrandom shape asymmetry between right and left femora unlikely (Ruff and Jones, 1981; Trinkaus et al., 1994). The seven samples were selected to represent the broadest possible range of time periods, geographic locations, and subsistence strategies. Individuals displaying indicators of obvious developmental pathology were excluded, although observations of nonspecific developmental stress (Harris lines, cribra orbitalia, and porotic hyperostosis) were not considered grounds for exclusion. Although detailed descriptions of these samples are published elsewhere (Cowgill, 2010), Table 1 includes samples sizes, sample locations, and general time periods for each skeletal sample.

Age was unknown for six of the seven samples used in this study, and crown and root formation evaluated from lateral mandibular radiographs was used whenever dental and postcranial remains were reliably associated. Crown and root formation was assessed following the developmental standards set by Smith (1991) for permanent dentition and Liversidge and Molleson (2004) for deciduous dentition. Each set of dentition was scored twice on two consecutive days, and individual teeth that produced different dental stage scores were evaluated a third time to resolve inconsistencies. When no dentition was directly associated with the postcranial remains, chronological age was predicted from within-sample Least Squares regression of femoral, tibial, or humeral length on age for each of the comparative samples to maximize sample size (Cowgill, 2010). By developing age-prediction equations specific to each sample, difficulties arising from the application of a formula developed

TABLE 1. Sample description, size, date, and location

Sample	Original location	Approximate time period	Sample size	Sample location
California Amerindian	Nothern California	500–4600 BP	91	Phoebe Hearst Museum at the University of California, Berkeley (Berkeley, CA)
Dart	Johannesburg South Africa	20th century	73	School of Medicine, University of Witwatersrand (Johannesburg, South Africa)
Indian Knoll	Green River, Kentucky	4143–6415 BP	95	University of Kentucky, Lexington (Lexington, KY)
Kulubnarti	Batn el Hajar, Upper Nubia	Medieval	99	University of Colorado, Boulder, (Boulder, CO)
Luis Lopes	Lisbon, Portugal	20th century	47	Bocage Museum (Lisbon, Portugal)
Mistihalj	Bosnia Herzegovina	Medievel (15th century)	52	Peabody Museum at Harvard University (Cambridge, MA)
Point Hope	Point Hope, Alaska	300–2100 BP	65	American Museum of Natural History (New York, NY)

on individuals differing in body size or proportions to an archaeological target sample are partially mitigated.

For the analysis of femoral shape, three variables were used: the ratio of maximum (I_{max}) to minimum (I_{min}) second moments of area, the ratio of AP (I_x) to ML (I_y) second moments of area, and theta (the orientation of maximum bending rigidity measured counterclockwise from the ML axis). Cross-sections were taken at the diaphyseal level that best approximates the 50% section level in fused, mature elements, when calculated from unfused biomechanical length following Trinkaus et al. (2002a, 2002b). In immature femora, the 50% level was calculated as 45.5% of femoral intermetaphyseal length, as this measurement best corresponds to the location of the 50% level in individuals with fused distal femoral epiphyses because of the relatively larger contribution of the distal epiphysis to biomechanical length in fused femora (Ruff, 2003b). Orientation of the element was similar to that of adults, using the linea aspera as a general guide for approximating the sagittal plane.

All cross-sectional properties were collected using a method similar to the "latex cast method" used by O'Neill and Ruff (2004) and the method used by Sakaue (1998), which rely on AP and ML radiographs and silicone molding putty. To reconstruct the femoral and humeral cross-sectional properties, the external surface of the diaphysis was molded with Cuttersil Putty Plus silicone molding putty. Anterior, posterior, medial, and lateral cortical bone widths were measured with digital calipers, and the measurements were corrected for parallax distortion by comparing external breadths measured on the radiograph with external breaths measured on the element. Once corrected for parallax, the four cortical bone measurements were plotted onto a two-dimensional copy of the original mold, and the endosteal contours were interpolated by using the subperiosteal outline as a guide. The resultant sections were enlarged on a digitizing tablet, and the endosteal and periosteal contours were digitized. Cross-sectional properties were computed from the sections in a PC-DOS version of SLICE (Nagurka and Hayes, 1980; Eschman, 1992).

The patterns in the ratios of I_x/I_y and I_{max}/I_{min} during the course of growth were evaluated through linear and curvilinear regression of these ratios on age, and the scatter plots of theta on age were used to explore change in the orientation of maximum bending rigidity.

Comparison of ground reaction force and structural geometry data

AP/ML GRF ratios were compared with cross-sectional I_x/I_y data. Spearman's rank correlation was used to determine the relationship between the AP/ML ratio and I_x/I_y ratios obtained from the skeletal data across four age categories (1.0–1.9 yr, 2.0–3.9 yr, 4.0–8.9 yr, and adults older than 18 yr).

RESULTS

Analysis of ground reaction forces

Young children produce greater ML and lower AP forces than adults (Fig. 1). Mean normalized peak medial force (peak ML/peak Z) was greatest in children aged 1.0–3.9 yr (mean 0.098, ± 0.022, n = 10), lower in children aged 4.0–8.9 yr (0.082 ± 0.022, n = 3), and lowest in adults (0.059 ± 0.013, n = 10). Means were significantly different between adults and the youngest children ($P < 0.001$) and between adults and children aged 4.0–8.9 yr ($P = 0.018$) but not between the two groups of children ($P = 0.145$). In contrast, normalized peak AP force (peak AP/peak Z) was similar for the youngest children (0.180 ± 0.057), older children (1.88 ± 0.019), and adults (0.222 ± 0.087, $P > 0.05$ all comparisons). A similar pattern was evident in comparisons of GRF impulse. Mean ML/Z impulse ratios were higher for the youngest children (0.063 ± 0.17) than for adults (0.038 ± 0.009, $P < 0.001$). ML/Z impulse ratios were intermediate for children 4.0–8.9 years (0.046 ± 0.022), but they were not significantly different from adults or younger children ($P > 0.05$ both comparisons). The ratio of AP/Z impulses was similar for the youngest children (0.104 ± 0.026), older children (0.113 ± 0.026), and adults (0.114, $P > 0.05$ all comparisons).

The ratio of peak AP to ML GRF (AP/ML) was significantly greater in adults (3.80 ± 1.05) than in children aged 1.0–3.9 yr (1.90 ± 0.60; $P < 0.001$) and children aged 4.0–8.9 yr (2.50 ± 0.71; $P = 0.025$) but not significantly different between the two groups of children ($P = 0.085$). Similarly, the ratio of AP/ML impulses was greater in adults (3.22 ± 0.60) than in the children aged 1.0–3.9 yr (1.76 ± 0.52; $P < 0.001$) and 4.0–8.9 yr (3.00 ± 1.66; $P = 0.024$), but the difference between the

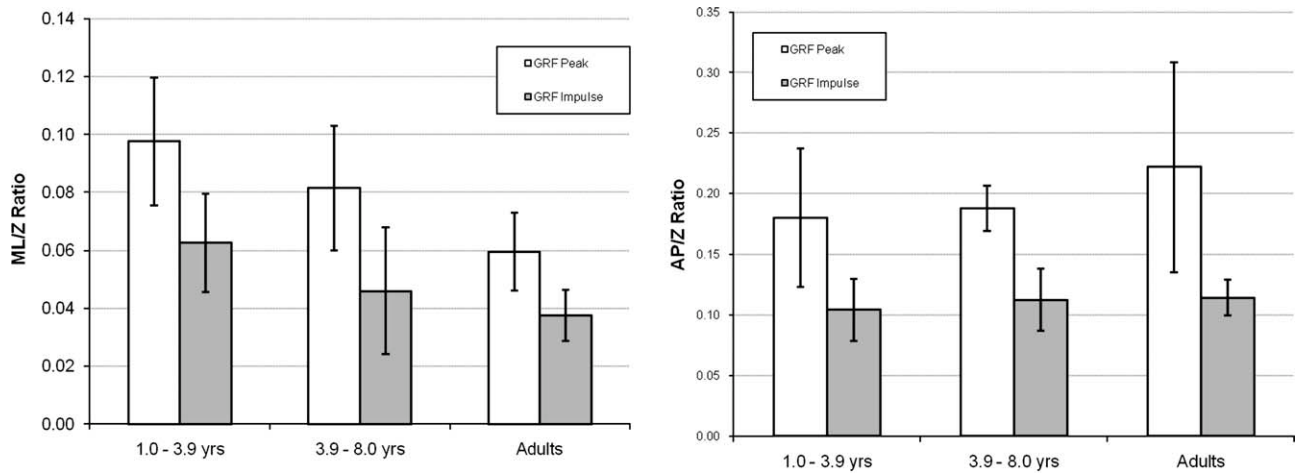

Fig. 1. (**a**) The ratio of ML/Z GRF in the three age categories. Young children (1.0–3.9 yr) and adults are significantly different ($P < 0.001$). (**b**) The ratio of AP/Z GRF in the three age categories. Error bars indicate one standard deviation from the mean.

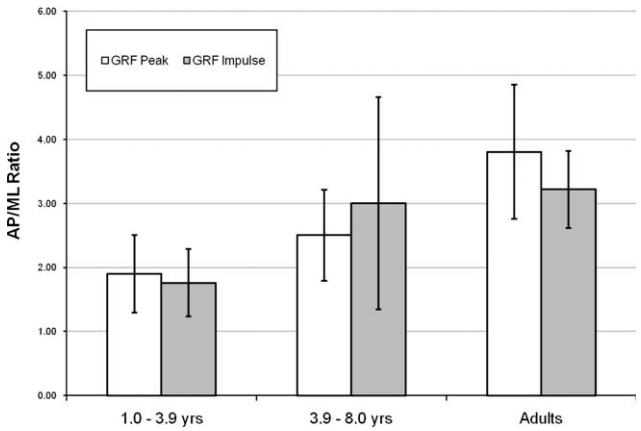

Fig. 2. The ratio of AP/ML GRF during walking for three age categories. Adults and young children (1.0–3.9 yr) are significantly different.

younger and older children was not significant ($P = 0.22$) (Fig. 2). These patterns were similar when all trials, including those in which velocity changed more than 20%, were included.

GRF patterns were notably more variable in young children than in older children and adults. Figure 3 shows ML and AP GRF traces relative to body weight for representative individuals in three age categories. Adult AP GRF traces show a well-characterized negative breaking force for the first 50% of stance, thereafter turning to a positive propulsive force for the second half of stance phase (Winter, 2005). The 4.0- to 8.9-yr-old age group shows a similar pattern, whereas the 1.0- to 3.9-yr-old age groups are the most variable. The youngest two individuals show large fluctuations in the first 50% of stance phase and a relatively low positive propulsive force at the end of stance phase. ML GRF patterns were less consistent for all subjects, but again the 1.0-to 3.9-yr old age groups are the most highly variable of the age groups.

These differences were not a function of differences in walking speed between groups. Froude number, a size-corrected speed, was similar for adults (0.197 ± 0.77), younger children (0.169 ± 0.082), and older children (0.160 ± 0.097; $P > 0.20$ all comparisons). Further, Froude number was not correlated with the ratio of AP/ML impulse ($r^2 = 0.04$, $P = 0.36$, ordinary least squares regression) nor with the ratio of peak AP/ML GRF ($r^2 = 0.01$, $P = 0.65$, Ordinary Least Squares (OLS)).

Limb segment angles were also broadly similar between adults and children. Limb excursion measured in the AP plane as the angle included by the ground plane and a line passing through the greater trochanter and lateral malleolus markers was similar at heel strike for children 1.0–3.9 years (108.2 ± 2.4°) and adults (108.5 ± 3.7°; p = 0.87), and at toe off (children: 59.5 ± 9.4°, adults: 61.4 ± 2.5°; $P = 0.54$). The lower limb was slightly more abducted in the ML plane at midstance for children. Limb adduction, measured as the angle of the line extending between the greater trochanter and later malleolus relative to vertical in the ML plane, was 1.6° greater in adults (8.3 ± 2.1°) than in young children (6.7 ± 1.1°; $P = 0.029$). Carrying angle, as the difference in orientation of the shank (knee-malleolus markers) and thigh (greater trochanter-knee markers) in the ML plane at midstance, was also greater in adults (3.2 ± 2.1°) than children (−0.4 ± 4.9°; $P = 0.024$). Note that the carrying angle measured here is taken from external landmarks not directly from skeletal measurements. Instead, the limb position seemed to be similar, with notable differences in the magnitude of AP and ML GRF (Fig. 4).

Analysis of midshaft femoral shape

Femoral I_x/I_y increases linearly with age, whereas the relationship between femoral I_{max}/I_{min} is best described with quadratic regression (Fig. 5). Early in growth, the ratio of AP to ML reinforcement is less than 1.0, indicating that femora have greater biomechanical reinforcement in a ML plane than in an AP one. In contrast, the ratio of maximum to minimum bending rigidity is as high in infancy as it is in adulthood, with cross-sections more closely approaching circularity in midchildhood. There is great variation in both ratios, however, which is possibly a result of pooling a wide variety of

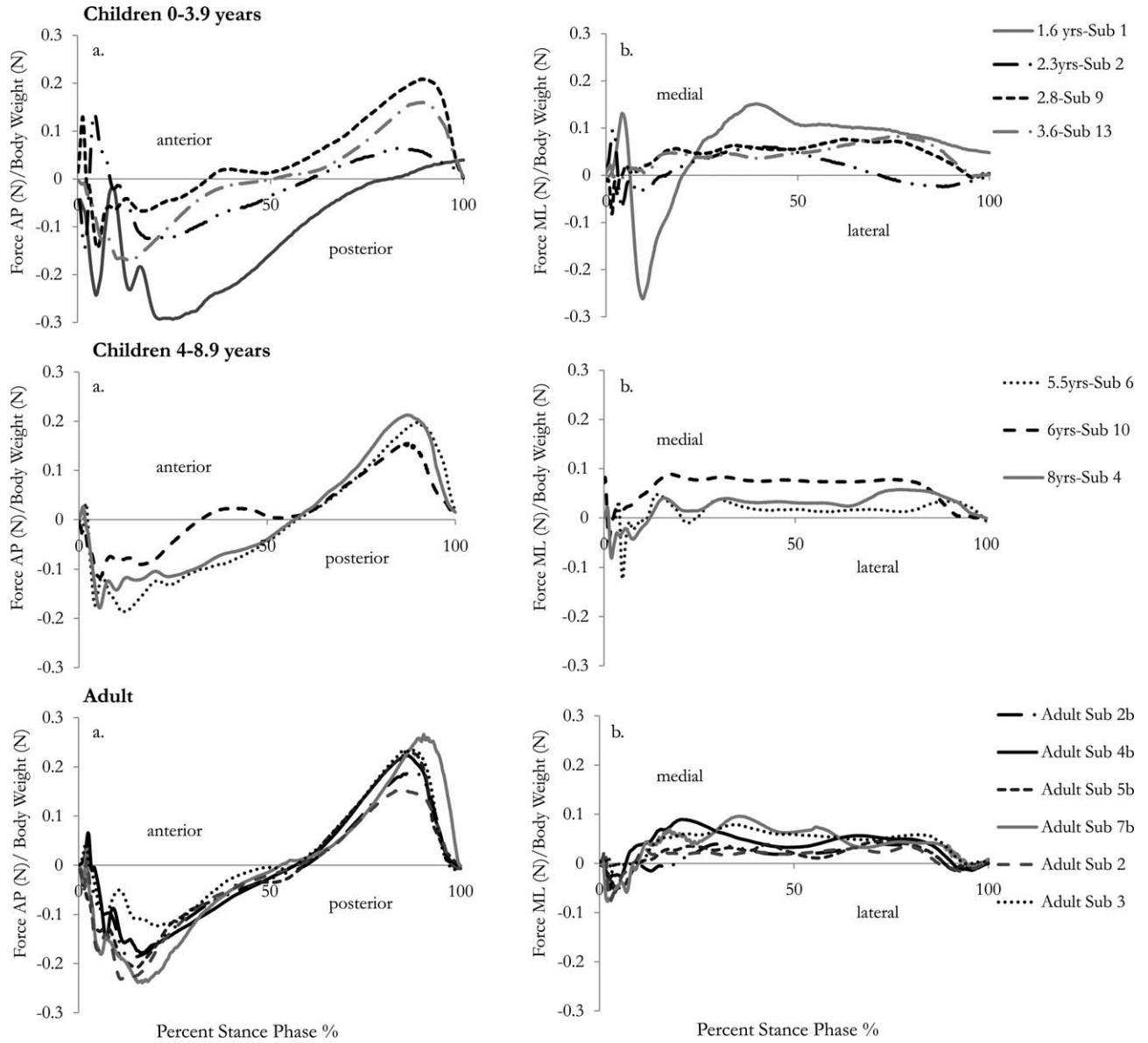

Fig. 3. (**a**) Anteroposterior and (**b**) mediolateral GRF trace relative to body weight in a representative sample of individuals from each age category. Shown as a percentage of stance phase. GRF traces are highly variable in the youngest age group (1.0–3.9 yr).

archeological samples of different temporal periods, geographic origins, and genetic backgrounds.

Age-specific means document similar trends to what is observed graphically (Table 2). Femoral I_x/I_y shows a slow increase in ratios, with generally overlapping confidence intervals, throughout the course of growth. Means for femoral I_x/I_y are less than 1.0 until the age of 6 yr; approximate adult values for femoral I_x/I_y are achieved between 12.0 and 13.9 yr of age. For femoral I_{max}/I_{min}, values between birth and 1.9 yr near those of adults. Femoral I_{max}/I_{min} means reach their nadir between 4.0 and 5.9 yr of age, and climb into late adolescence thereafter.

The changes also occur during growth in the orientation of maximum bending rigidity. Figure 6 shows a scatterplot of theta for both the right and the left femora during growth, where the orientation of maximum bending rigidity in left-side elements has been converted to that of right-side elements (e.g. 180°—Left Femur Theta). Early in development, the orientation of maximum bending rigidity is approximately medio-lateral. This is followed by a period of variation until, approximately at the age of 12 yr, the orientation of maximum bending rigidity becomes more anteroposteriorly oriented, corresponding with the orientation of the femoral pilaster.

Figure 7 illustrates this pattern using a generalized schematic diagram of the femoral cross-section of a 2-year old and a 16-year old children, where the ratios of I_{max}/I_{min} are similar. Even at this young age, the femoral cross-section of a 2-year old children is not purely circular, but heavily reinforced in an approximately ML plane.

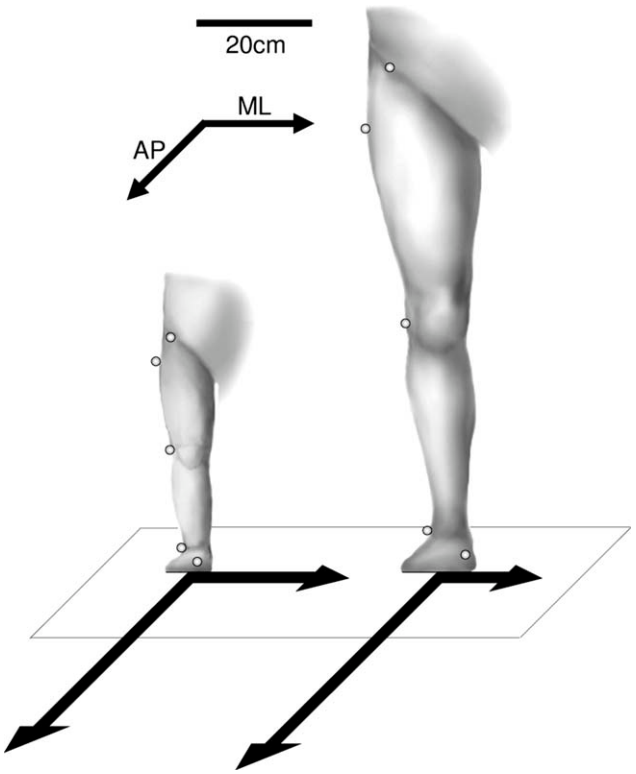

Fig. 4. The positions of the anterior iliac spine, greater trochanter, lateral femoral condyle, later maleolus, and hallux markers in the ML plane at mid-distance for a representative child and adult subject. Arrows indicate mean ML/Z and AP/Z GRF impulse ratios for young children (1.0–3.9 yr) and adults, respectively. Note that lower limb abduction and carrying angle are broadly similar but with slightly less adduction in children.

Comparison of ground reaction force and structural geometry data

When AP/ML GRF ratio is compared with I_x/I_y ratio of femoral shape using the four age group means, there is a strong positive correlation between I_x/I_y and AP/ML ratio ($\rho = 0.758$). Figure 8 shows the relationship between mean femoral I_x/I_y values and mean peak AP/ML GRF ratios in the four age categories. As ML GRF decreases across growth, so does ML reinforcement of the midshaft femur.

DISCUSSION

The results of this analysis support the idea that immature gait engenders high ML loads and that the immature femur responds to these loads through changes in shape. Despite the relatively small sample size, the GRF data indicate that bending loads placed on the lower limb differ between children and adults in their orientation and relative magnitude. ML forces are significantly higher in young children than in adults, and although not statistically significantly different, children between the ages of 4 and 8 years seem to be intermediate in their ML forces. AP ground forces are similar in children and adults, and as a result, the bending regime experienced by the lower limb seems to differ between children and adults, with young children experiencing a significantly lower ratio of AP/ML bending.

One important limitation of our analysis is that we did not calculate bending moments for the femur, and instead examined only ground forces. Forces recorded at the ground plane (i.e., by a force plate) are separated from the femur by considerable distance and at least three skeletal elements; GRF traces must, therefore, be considered indirect evidence for the actual bending moments experienced by the femur. Calculating bending

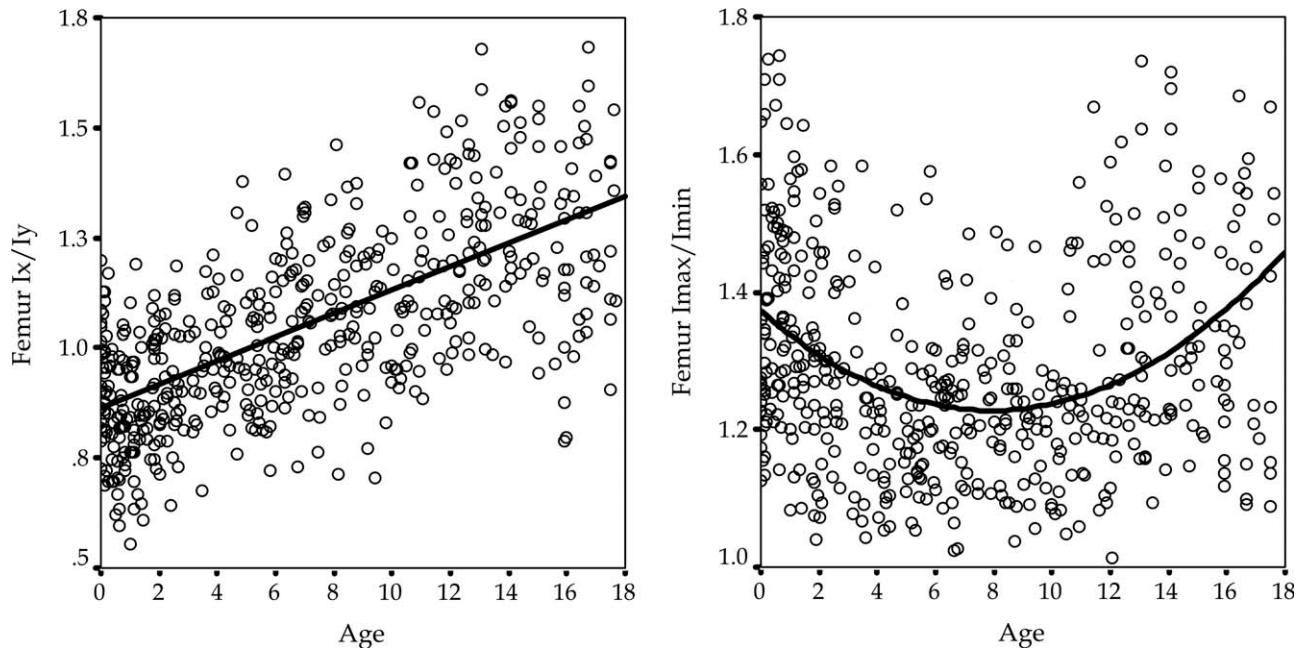

Fig. 5. Linear and quadratic regressions of femoral I_x/I_y ($y = 0.863 + 0.027x$, $r^2 = 0.402$, N = 521, $P < 0.001$) and I_{max}/I_{min} ($y = 1.371 - 0.036x + 0.002x^2$, $r^2 = 0.118$, N = 518, $P < 0.001$) on age.

TABLE 2. Age specific means for femoral shape ratios

		Femur Ix/Iy	Femur Imax/Imin
	N	135	134
0.0–1.9 yr	Mean	0.879	1.353
	95% CI	0.845–0.898	1.325–1.386
	N	58	58
2.0–3.9 yr	Mean	0.933	1.294
	CI	0.900–0.978	1.250–1.340
	N	60	60
4.0–5.9 yr	Mean	0.982	1.208
	95% CI	0.949–1.030	1.170–1.244
	N	54	54
6.0–7.9 yr	Mean	1.072	1.236
	95% CI	1.031–1.117	1.207–1.268
	N	48	47
8.0–9.9 yr	Mean	1.096	1.217
	95% CI	1.028–1.127	1.181–1.249
	N	49	48
10.0–11.9 yr	Mean	1.171	1.262
	95% CI	1.105–1.228	1.218–1.321
	N	46	46
12.0–13.9 yr	Mean	1.246	1.318
	95% CI	1.205–1.334	1.268–1.386
	N	40	40
14.0–15.9 yr	Mean	1.250	1.344
	95% CI	1.189–1.311	1.295–1.394
	N	33	32
16.0–17.9 yr	Mean	1.284	1.384
	95% CI	1.167–1.331	1.294–1.456

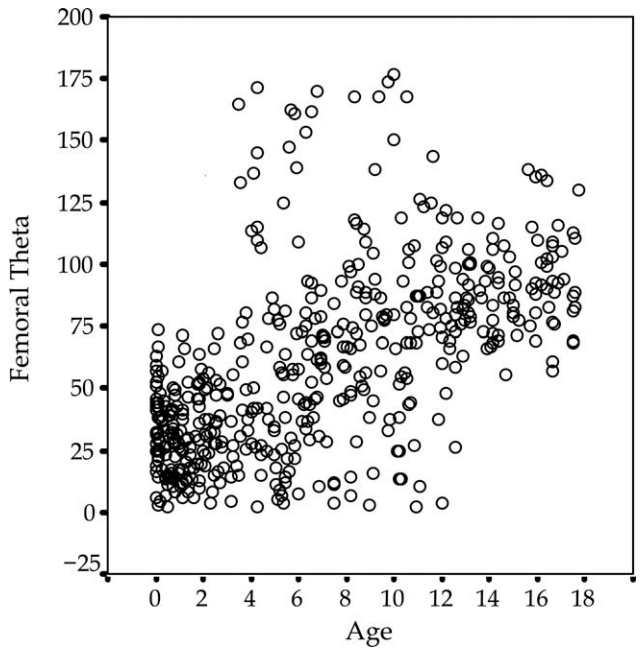

Fig. 6. Orientation of maximum femoral bending rigidity measured counterclockwise from the mediolateral axis (in degrees) on age.

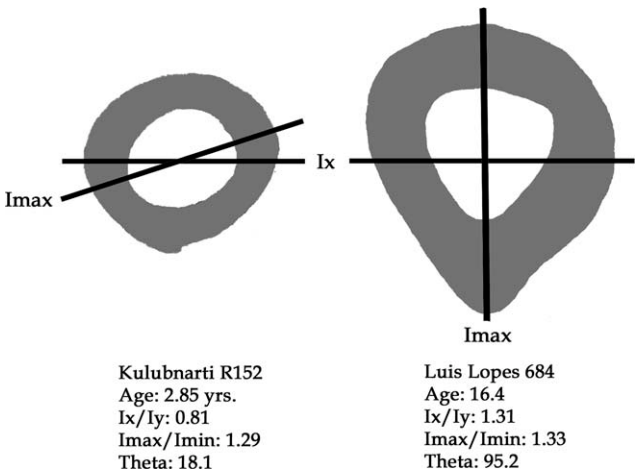

Fig. 7. Diagram of the midshaft femoral cross-section of a 2-year-old and a 16-year-old children. In both individuals, I_{max}/I_{min} is similar, but the orientation of maximum bending rigidity differs.

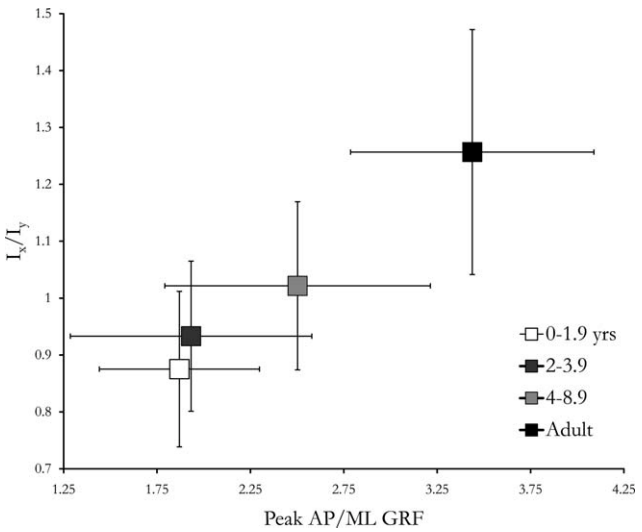

Fig. 8. Mean femur Ix/Iy values versus mean peak AP/ML GRF ratios for four age categories. Mean femoral shape ratio and GRF ratios are positively correlated ($\rho = 0.758$). Error bars represent one standard deviation on both axes.

moments for the femur would require either a validated finite element model for the lower limb, or, at minimum, precise information on the location of the skeletal elements relative to external reflective markers in both the AP and the ML planes. This latter consideration is not negligible, particularly for young children in whom substantial subcutaneous fat lies between the external reflective markers and femur. Future work might employ finite element modeling or more detailed kinematic and anatomical data to calculate femoral bending moments directly, rather than examining the indirect indices of bending moments used here.

Ontogenetic changes in femoral strength

Differences between children and adults in the relative level of ML bending force seem to be reflected in changes in femoral geometry during growth. Early in growth, the midshaft femur is heavily reinforced in an approximately ML plane. The ratio of maximum to minimum bending rigidity in a toddler is similar in magnitude to that of an adult. However, the orientation of maximum bending rigidity in an early walker differs from that of an

adult: where adults possess anteroposteriorly elongated midshaft femoral cross-sections, the femoral cross-section of a young walker is reinforced mediolaterally.

Previous research has demonstrated that immature bone responds rapidly to changing biomechanical environments (Steinberg and Trueta, 1981; Raab et al., 1990). For example, Lieberman et al. (2001) demonstrated that bone in juvenile sheep responds more strongly to mechanical stress than does the bone in adults. In addition, Ruff (2003a, 2003b) detected early changes in the femoral and humeral strength proportions that are best explained as a result of the initiation of upright walking. In a study of growth velocities of the immature human femur and humerus, femoral growth velocity displayed a peak in infancy, with a mean age of peak at 1.4 years. Humeral growth velocity exhibited a similar peak slightly earlier (1.1 years of age), followed by a steep decline. This femoral peak seems to correspond to the initiation of bipedal walking. The humeral peak and subsequent decrease in growth velocity is likely a result of the shift from crawling, where it is used as a weight-bearing element, to independent standing and walking, where the humerus assumes a more manipulative role (Ruff, 2003b). These "infancy peaks" illustrate both that immature bone responds rapidly to changes in loading regime and that these responses can be detected through the analysis of cross-sectional geometry. Given the highly responsive nature of juvenile bone, it seems unlikely that the ML femoral reinforcement detected in this analysis is simply the biological default shape for the immature femoral midshaft, as it seems to be actively maintained until midchildhood.

Explaining GRF patterns in young children

Which differences in gait or anatomy lead to increased ML ground forces in children relative to adults? Several plausible explanations exist, although they are not mutually exclusive. One possibility is that children use an inefficient control regime that produces greater ML forces than are necessary to maintain balance. Young children might use a gait with greater ML force production either because of a lack of motor control development or because energy efficiency is not their primary performance criterion. There is some support for this hypothesis; studies of locomotor cost and mechanical work during walking in children have shown that children under the age of 5 years are mechanically inefficient and metabolically costly compared with adults (DeJaeger et al., 2001; Scheppens et al., 2004).

Two alternative hypotheses focus on differences in the body proportions and lower limb anatomy between children and adults that could lead to differences in GRF patterning and bending regimes. First, children have short lower limbs and wide trunks compared with adults (Robbins et al., 1928; Knott and Meredith, 1937), requiring greater hind limb adduction to place the foot directly below the body's center of mass during single-foot support in walking. Instead, as evident in our analyses, children use a slightly less adducted hind limb at midstance; the lack of adduction is exacerbated by the lack of a bicondylar angle in young children. As a result, young children must generate greater ML forces than adults to maintain balance.

Rapid postnatal growth of the lower limb relative to hip breadth results in dramatically changing body proportions during the course of human ontogeny, as the human form transitions from the relatively stocky build of young children to the more linear body of adolescents. Femoral cross-sectional shape has been shown to be sensitive to differences in body form in adult modern humans and fossil hominins, primarily through changes in mechanical loading around the hip joint (Ruff, 1995; Ruff et al., 2006). ML bending loads (and thereby ML reinforcement of the femoral diaphysis) increase as pelvic width relative to femoral length increases (Ruff et al., 2006). Therefore, it is possible that the high level of femoral ML buttressing detected in young walkers is a consequence of their broad pelves relative to the lower limb length.

Second, as is evident in our analyses and others (McGraw, 1940; Okamoto and Okamoto, 2007), children have a slightly abducted lower limb at midstance, which may be caused by a minimally developed bicondylar angle. The femoral bicondylar angle is a developmentally plastic feature of the distal femur, caused by differential growth between the lateral and medial sides of the distal femoral metaphysis (Shefelbine et al., 2002). Under normal loading conditions, the bicondylar angle reaches adult values (8–11°) between the ages of 4 and 8 years (Tardieu and Trinkaus, 1994; Shefelbine et al., 2002). The ultimate effect of a femoral bicondylar angle in modern humans is to adduct the knee, thereby positioning the knee closer to the sagittal plane, under the body's center of gravity during bipedal locomotion (Tardieu and Trinkaus, 1994). The relatively wide stance observed in young children, which partially creates the appearance of a "waddling" gait in toddlers, is likely related to minimal development of the bicondylar angle. Combined with a relatively broad pelvis for height, young children would actually need rather large bicondylar angles to be more functionally equivalent to adults, as is seen in some early hominins with broad pelves (Tardieu and Trinkaus, 1994).

A wide stance, an abducted limb, and a waddling gait have been linked to high ML forces in several animals, including penguins (Griffen and Kram, 2000), alligators (Blob and Biewener, 1999, 2001), lemurs (Carlson, 2005), mice (Carlson and Judex, 2007), and extinct taxa (Jungers and Minns, 1979). Penguins, in particular, the consummate "waddlers" of the animal kingdom, generate ML forces that are very high when compared with other vertebrates (Griffen and Kram, 2000). Nakatsukasa et al. (1995) examined the cross-sectional properties of a Japanese macaque that had been trained to walk bipedally during the course of 11 years, starting at 3 years. No bicondylar angle had developed (likely because of the developmentally late adoption of bipedalism), and analysis of gait pattern in this individual confirmed that the macaque walked bipedally with an abducted thigh. Contrary to expectations, analysis of midshaft femoral cross-sectional properties did not find that the femur was reinforced in an AP plane; the orientation of maximum bending rigidity was approximately ML at 18.7°, an angle similar to the maximum bending rigidity orientation observed here in a large sample of immature children. These authors interpreted these differences as a result of fundamental differences between macaque and human bipedalism, principally related to the abduction of the thigh during bipedality. Failure to position the knee near the body's center of mass via a well-developed bicondylar angle may further increase ML bending around the femoral diaphysis.

CONCLUSIONS

The extent to which greater ML ground forces are a function of differences in body proportions, skeletal anatomy, or inefficient motor control in children warrants further investigation. However, our results suggest that the anatomical differences between children and adults increase ML bending moments around the femoral midshaft and affect diaphyseal shape in young walkers. The vast majority of developmental studies have tended to view the immature human skeleton as progressing toward a single endpoint: the mature adult morphology. However, it is possible that the developing skeleton moves through distinct biomechanical and morphological phases that are unique to the growth period. In this context, the relatively rounder shafts of young individuals should not be viewed as a product of the absence of biomechanical loading, but as an early functional adaptation to the unusual demands of "waddling" locomotion.

ACKNOWLEDGMENTS

We thank E Trinkaus, CB Ruff, G Conroy, C Hildebolt, and R Smith for their assistance and advice throughout the course of this project. We also thank the reviewers that made many helpful comments on this article.

LITERATURE CITED

Alexander RM. 1984. The gaits of bipedal and quadrupedal animals. Int J Robotics Res 3:49–59.

Blob RW, Biewener AA. 1999. In vivo locomotor strain in the hindlimb bones of *Alligator mississippiensis* and *Iguana iguana*: implications for the evolution of limb bone safety factor and non-sprawling limb posture. J Exp Biol 202:1023–1046.

Blob RW, Biewener AA. 2001. Mechanics of limb bone loading during terrestrial locomotion in the green iguana (*Iguana iguana*) and American alligator (*Alligator mississippiensis*). J Exp Biol 204:1099–1122.

Carlson KJ. 2005. Modeling arboreal locomotion: the effect of limb abduction on substrate reaction forces during lemurid quadrupedal locomotion. Integr Comp Biol 45:974.

Carlson KJ, Judex S. 2007. Increased non-linear locomotion alters diaphyseal bone shape. J Exp Biol 210:3117–3125.

Carriero A, Zavatsky A, Stebbins J, Theologis T, Shefelbine SJ. 2009. Correlation between lower limb bone morphology and gait characteristics in children with spastic diplegic cerebral palsy. J Pediatr Orthop 29:73–79.

Cowgill LW. 2010. The ontogeny of Holocene and Late Pleistocene human postcranial strength. Am J Phys Anthropol 141: 16–37.

DeJaeger D, Willems PA, Heglund NC. 2001. The energy cost of walking in children. Eur J Physiol 441:538–543.

Eschman PN. 1992. SLCOMM Version 1.6. Albuquerque, NM: Eschman Archaeological Services.

Griffin TM, Kram R. 2000. Penguin waddling is not wasteful. Nature 408:929.

Holt BM. 2003. Mobility in upper paleolithic and mesolithic europe: evidence from the lower limb. Am J Phys Anthropol 122:200–215.

Jungers WL, Minns RJ. 1979. Computed tomography and biomechanical analysis of fossil long bones. Am J Phys Anthropol 50:285–290.

Knott VB, Meredith HV. 1937. Changes in body proportions during infancy and the preschool years. II. Width of hips in relation to shoulder width, chest width, stem length, and leg length. Child Dev 8:311–327.

Lanyon LE, Hampson WGJ, Goodship AE, Shah JS. 1975. Bone deformation recorded from strain gauges attached to the human tibial shaft. Acta Orthop Scan 46:256–268.

Larsen CS. 1997. Bioarchaeology: interpreting behavior from the human skeleton. New York: Cambridge University Press.

Lieberman DE, Devlin MJ, Pearson OM. 2001. Articular area responses to mechanical loading: effects of exercise, age, and skeletal location. Am J Phys Anthropol 116:266–277.

Liversidge HM, Molleson T. 2004. Variation in crown and root formation and eruption of human deciduous teeth. Am J Phys Anthropol 123:172–180.

McGraw MB. 1940. Neuromuscular development of the human infant as exemplified in the achievement of erect locomotion. J Pediatr 17:747–771.

Morrison JB. 1969. Function of the knee joint in various activities. Biomed Eng 4:573–580.

Nagurka ML Hayes WC. 1980. An interactive graphics package for calculating cross sectional properties of complex shapes. J Biomech 13:59–64.

Nakatsukasa M, Hayama S, Preuschoft H. 1995. Postcranial skeleton of a macaque trained for bipedal standing and walking and implications for functional adaptation. Folia Primatol 64:1–29.

Okamoto T, Okamoto K. 2007. Development of gait by electromyography. Osaka: Walking Development Group.

O'Neill MC, Ruff CB. 2004. Estimating human long bone cross-sectional geometric properties: a comparison of noninvasive methods. J Hum Evol 47:221–235.

Paul JP. 1971. Load actions on the human femur in walking and some resultant stresses. Exp Mech 11:121–151.

Pontzer H. 2005. A new model predicting locomotor cost from limb length via force production. J Exper Biol 208:1513–1524.

Raab DM, Smith EL, Crenshaw TD, Thomas DP. 1990. Bone mechanical properties after exercise training in young and old rats. J Appl Physiol 68:130–134.

Richmond BG, Jungers WL. 2008. Orrorin tugenensis femoral morphology and the evolution of hominin bipedalism. Science 319:1662–1665.

Robbins WJ, Brody S, Hogan AG, Jackson CM, Greene CW. 1928. Growth. New Haven: Yale University Press.

Ruff CB. 1987. Sexual dimorphism in human lower limb bone structure: relationship to subsistence strategy and sexual division of labor. J Hum Evol 16:391–416.

Ruff CB. 1995. Biomechanics of the hip and birth in early Homo. Am J Phys Anthropol 98:527–574.

Ruff CB. 2000. Biomechanical analyses of archaeological human skeletons. In: Katzenberg MA, Saunders SR, editors. Biological anthropology of the human skeleton. New York: Wiley-Liss. p 71–102.

Ruff CB. 2003a. Ontogenetic adaptation to bipedalism: age changes in femoral to humeral length and strength proportions in humans, with a comparison to baboons. J Hum Evol 45:317–349.

Ruff CB. 2003b. Growth in bone strength, body size, and muscle size in a juvenile longitudinal sample. Bone 33:317–329.

Ruff CB, Holt BM, Sladek V, Berner M, Murphy Jr WA, Nedden DZ, Seidler H, Recheis W. 2006. Body size, body proportions, and mobility in the Tyrolean "Iceman." J Hum Evol 51:91–101.

Ruff CB, Jones HH. 1981. Bilateral asymmetry in the cortical bone of the humerus and tibia- sex and age factors. Hum Biol 53:69–86.

Sakaue K. 1998. Bilateral asymmetry of the humerus in Jomon people and modern Japanese. Anthropol Sci 105:231–246.

Schepens B, Bastien GJ, Heglund NC, Willems PA. 2004. Mechanical work and muscular efficiency in walking children. J Exper Biol 207:587–596.

Shackelford LL. 2007. Regional variation in the postcranial robusticity of late Upper Paleolithic humans. Am J Phys Anthropol 133:655–668.

Shaw CN, Stock JT. 2009. Intensity, repetitiveness, and directionality of habitual adolescent mobility patterns influence the tibial diaphysis morphology of athletes. Am J Phys Anthropol 140:149–159.

Shefflbine SL, Tardieu C, Carter DR. 2002. Development of the femoral bicondylar angle in hominid bipedalism. Bone 30: 765–770.

Smith BH. 1991. Standards of human tooth formation and dental age assessment. In: Kelley MA, Larsen CS, editors. Advances in dental anthropology. New York: Wiley-Liss. p 143–168.

Statham L, Murray MP. 1971. Early walking patterns of normal children. Clin Orthop 79:8–24.

Steinberg ME, Trueta J. 1981. Effects of activity on bone growth and development of the rat. Clin Orthop Relat R 156:52–60.

Stock JT, Pfeiffer SK. 2001. Linking structural variability in long bone diaphyses to habitual behaviors: foragers from the Southern African Later Stone Age and the Andaman Islands. Am J Phys Anthropol 115:337–348.

Stock JT, Pfeiffer SK. 2004. Long bone robusticity and subsistence behavior among Later Stone Age foragers of the forest and fymbos biomes of South Africa. J Archaeol Sci 31:999–1013.

Sutherland DH, Olshen R, Cooper L, Woo SL-Y. 1980. The development of mature gait. J Bone Joint Surg 62:336–353.

Sutherland DH, Olshen R, Biden EN, Wyatt MP. 1988. The development of mature walking. Philadelphia: Mac Keith Press.

Tardieu C, Trinkaus E. 1994. Early ontogeny of the human femoral bicondylar angle. Am J Phys Anthropol 95:183–195.

Trinkaus E. 1997. Appendicular robusticity and the paleobiology of modern human emergence. Proc Natl Acad Sci USA 94: 13367–13373.

Trinkaus E, Churchill SE, Ruff CB. 1994. Postcranial robusticity in Homo. II. Humeral bilateral asymmetry and bone plasticity. Am J Phys Anthropol 93:1–34.

Trinkaus E, Ruff CB, Esteves F, Coelho JMS, Silva M, Mendova M. 2002a. The lower limb remains. In: Zilhão J, Trinkaus E, editors. Portrait of the artist as a child. Lisbon: Intituto Português de Arqueologia. p 435–465.

Trinkaus E, Ruff CB, Esteves F, Coelho JMS, Silva M, Mendova M. 2002b. The upper limb remains. In: Zilhão J, Trinkaus E, editors. Portrait of the artist as a child. Lisbon: Intituto Português de Arqueologia. p 466–488.

Wescott DJ. 2006. Effect of mobility on femur midshaft external shape and robusticity. Am J Phys Anthropol 130:201–213.

Winter D. 2005. Biomechanics and motor control of human movement. Hoboken: John Wiley and Sons, Inc.